CHAPTER V

APPLICATION EXAMPLES OF THE PROPOSED SWITCHING FLOW-GRAPH MODEL

5.1 Introduction

There are several application examples discussed in this chapter. In section 5.2, the proposed SFG model of the inverters is applied to join with the motor system to execute the time-domain simulation. In the first example, the SFG model is worked with the PSB (Power System Blockset of MATLAB/SIMULINK) functional blocks for the purpose of fast simulation. In the second example, the simulation structure for a surface mounted permanent magnet synchronous motor (SMPMSM) driven by the proposed SFG model of inverter is demonstrated. It introduces how to use the steady-state model to observe the working points. The simple PI-controllers are also designed to control the phase currents and to regulate the rotor speed of the SMPMSM by using the small-signal model. This example also demonstrates how to establish a completed simulation structure at system-level with using the proposed SFG model. From these examples, one can perceive that the proposed SFG models are very feasible analysis and design of three-phase switching system. It is also easy to connect the proposed SFG model with other subsystem to complete a system-level simulation.

In section 5.3, the example of controller design for the three-phase rectifiers based on the proposed SFG model is illustrated. The concept of internal model control (IMC) is engaged to quickly create the PI-controllers. This example reveals the procedures of controller design by using the proposed SFG model of the rectifiers. This example shows that the controller design becomes straightforward and the

difficult mathematics is evitable by using the proposed SFG model.

5.2 Application Examples of Inverters

5.2.1 Simulation Examples by Using the Proposed SFG Model

Example A

In this example, the proposed SFG model is worked with the PSB (Power System Blockset of MATLAB/SIMULINK) functional blocks. There are many well-known circuit topologies and motor models created in this toolbox. This example introduces how to use the proposed SFG model of inverter to connect with the PSB functional blocks to fast simulate the motor system.

Consider a three-phase industrial motor rated 3 HP, 220 V, and 1725 rpm as an example. The block of the "Asynchronous Machine SI Units", built in PSB, is used to be the simulation model of the motor. The proposed SFG model of the inverter, as shown in Fig. 3.5, is used to drive the motor. The simulation condition includes (the demonstration example is also supplied in PSB/SIMULINK/MATLAB):

stator resistance $R_S = 0.435\Omega$, leakage inductance $L_{lS} = 2mH$,

rotor resistance $R'_r = 0.816\Omega$, leakage inductance $L'_{lr} = 2mH$

mutual inductance $L_m = 69.31mH$,

number of poles $P = 4$,

$V_{LL} = 220V$, switching frequency $f_S = 1kHz$

Base frequency $f_n = 60Hz$

Inertia $J = 0.089 \quad kg.m^2$

The load torque applied to the machine's shaft is constant and set to be 11.87 N.m.

The structure of the simulation system is shown in Fig. 5.1. One can see that when the proposed SFG model of the inverter is connected with the motor model

represented as the block of “Asynchronous Machine SI Units”, the functional blocks of “ASM Measurement Demux”, “Controlled Voltage Source” and “Voltage Measurement” should be added. In this case, the blanking-time and R_{ON} of the switches are set to be zero. The motor is started from zero speed and the original speed is set to *0.5p.u.*. Then, the speed setpoint is stepped to *0.75p.u.* at $t = 1sec.$ Fig. 5.2 shows the simulation waveforms of the stators currents (*A*), mechanical rotor speed (*rad/s*) and electromagnetic torque (*N.m*). From Fig. 5.2, one can find the rotor speed reaches 827 *rpm* after 0.8*sec* and stabilizes at 1270 *rpm.* The simulation results generated by using the proposed SFG model are well confirmed with the results generated from the demonstration example supplied by MATLAB/SIMULINK software.

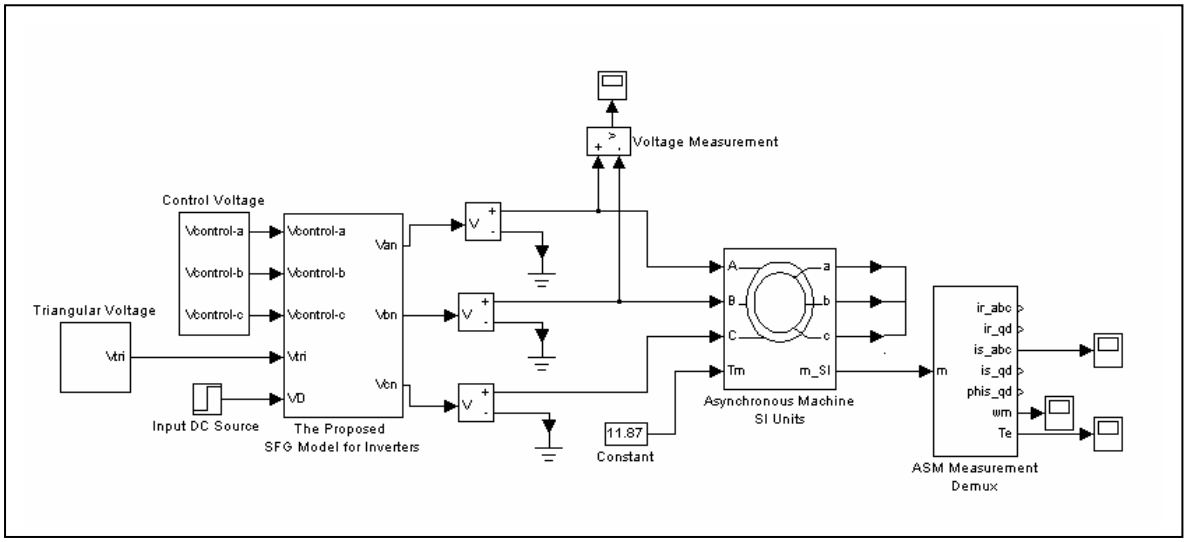

Fig. 5.1 The simulation structure of the proposed SFG model connecting with the functional blocks of PSB.

The simulation structure described in Fig. 5.1 is suitable for simple evaluation of a motor system with open-loop control. However, when the blanking-time effect is considered or simulation with the closed-loop control, the problems of the divergence maybe occur. That is because the simulation signals are sampled and feed back to the control system that may cause the singular points during running the algebraic loops inner the functional blocks of PSB. This is an existent problem of the PSB.

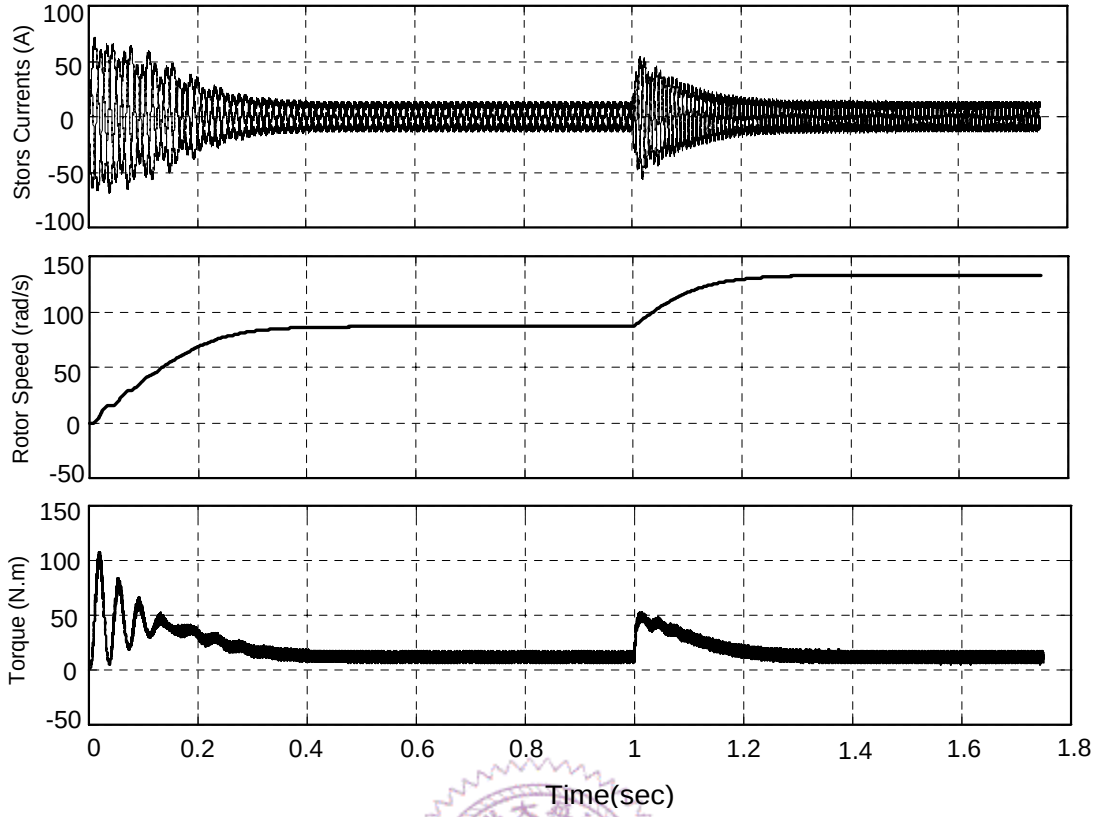

Fig. 5.2 The simulation waveforms of stators currents (*A*), mechanical rotor speed (*rad/s*) and electromagnetic torque (*N.m*).

Example B

The simulation structure for a surface mounted permanent magnet synchronous motor (SMPMSM) driven by the proposed SFG model of inverter is demonstrated in this example. In order to prevent the problem of the divergence, the simulation model of SMPMSM is created with SIMULINK without using the PSB.

Consider the SMPMSM which parameters are shown in the following [44]:

Resistance $R_S = 3.55\Omega$, Inductance $L_S = 5.92mH$,

Number of poles $P = 8$, Flux-linkage $\lambda_f = 0.0579\ V/(rad/s)$,

Rotor inertia $J_m = 6.45e-5\ \ kg.m^2$,

Friction factor $B_m = 8e-5\ \ N.m.s/rad$,

$V_D = 135V$, Switching frequency $f_S = 1kHz$,

Base frequency $f_n = 40Hz$, Blanking time $10\mu s$.

The mathematical model of the SMPMSM drive system in the synchronous reference frame can be described as follows [45]:

$$v_{ds} = R_s i_{ds} + \frac{d}{dt}\lambda_{ds} - \omega_r \lambda_{qs} \tag{5.1}$$

$$v_{qs} = R_s i_{qs} + \frac{d}{dt}\lambda_{qs} + \omega_r \lambda_{ds} \tag{5.2}$$

$$\lambda_{ds} = L_s i_{ds} + \lambda_f i_{qs} \tag{5.3}$$

$$\lambda_{qs} = L_s i_{qs} \tag{5.4}$$

$$T_e = \frac{3}{2}\frac{P}{2}\lambda_f \tag{5.5}$$

where $v_{ds}\_v_{qs}$, $i_{ds}\_i_{qs}$, and $\lambda_{ds}\_\lambda_{qs}$ denote the stator d_q axis voltages, currents and flux linkages, respectively; λ_f is the flux linkage due to the permanent magnet. The rotor speed and electromagnetic torque are represented as ω_r and T_e; and R_s, L_s and P are the stator resistance, stator inductance and the number of poles, respectively.

According to the dynamic equations, described in equations (5.1) ~ (5.5), one can create the simulation model of the SMPMSM with SIMULINK /MATLAB as shown in Fig. 5.3. As the proposed SFG model of the inverters is used to drive the SMPMSM, the simulation structure can be depicted in Fig. 5.4. In Fig. 5.4, the proposed SFG model of the inverters is created according to Fig. 3.11.

In this case the SMPMSM is started from zero speed and the original speed-command is +1800 *rmp*. Then the speed-command is changing to -1800 *rpm* at 0.15 *sec*. The simulation results are shown in Fig. 5.5. Because this example is under the open-loop control, one can observe that the rotor speed is damped around the input demand.

This example demonstrates how to establish the open-loop control structure for simulation of a motor system with the proposed SFG model. The blank-time effect and the ON-resistance of active switches are both considered and there is no problem of divergence. Next section will discuss the construction of the closed-loop control

structure for simulation of a motor system with the proposed SFG model.

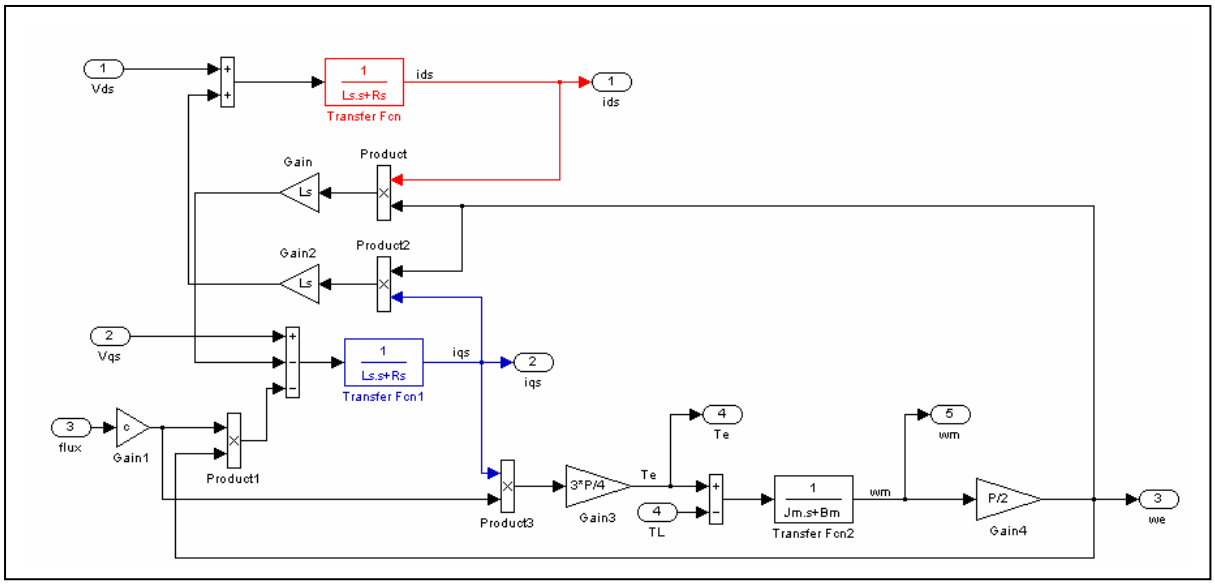

Fig. 5.3 The simulation model of the SMPMSM implemented with MATLAB/SIMULINK.

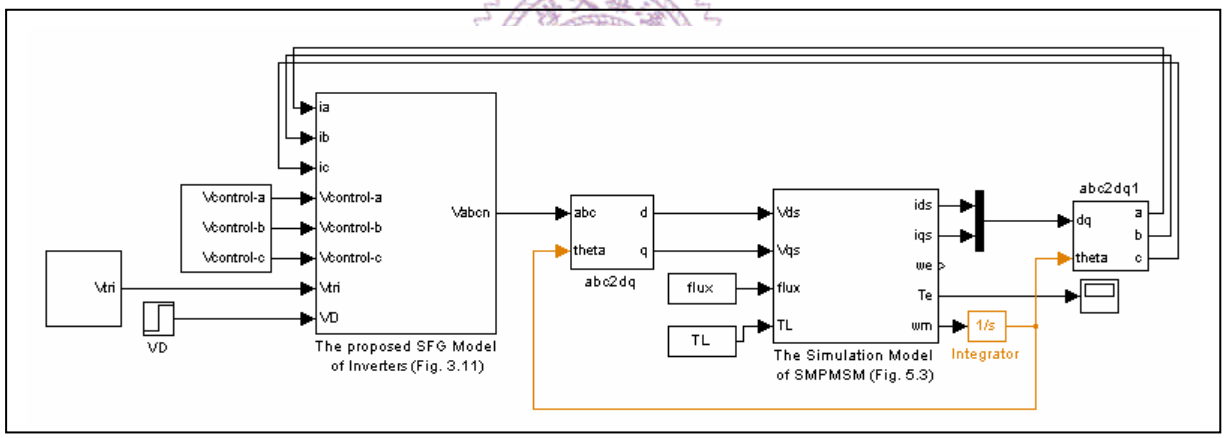

Fig. 5.4 The simulation structure of the SMPMSM with MATLAB/SIMULINK.

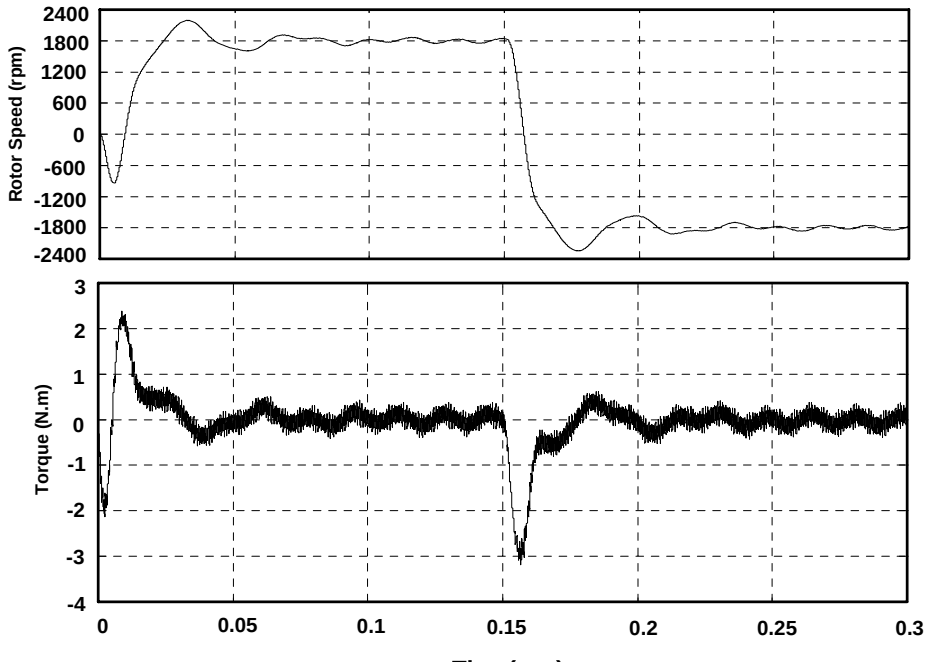

Fig. 5.5 The simulation waveforms of torque and rotor speed.

5.2.2 Design Examples by Using the Proposed SFG Model

In this section, the same SMPMSM introduced in 5.2.1 Example B is used as the example. This section introduces how to design the controllers based on the small-signal model.

Fig. 5.10 shows the control structure of the SMPMSM. The speed controller and the bound calculator are designed by following the concept of field weakening control strategies in [44].

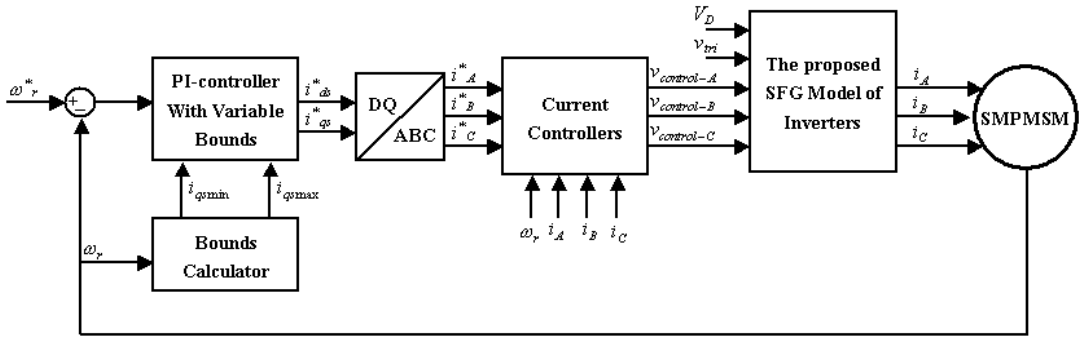

Fig. 5.6 The control structure of the SMPMSM.

According to the small-signal model as described in Fig. 3.7, one can neglect the nonlinear terms and reconstruct the small-signal model in frequency domain. Fig. 5.11 shows the small-signal model represented in frequency-domain, where the $\hat{v}_{Dj}(s)$ means the Lapalce transform of $D_j(t)\hat{v}_D(t)$ as described in equation (5.8).

$$\hat{v}_{Dj}(s) = \mathrm{L}\left(D_j(t)\hat{v}_D(t)\right) \qquad for \quad j \in \{A,B,C\} \tag{5.6}$$

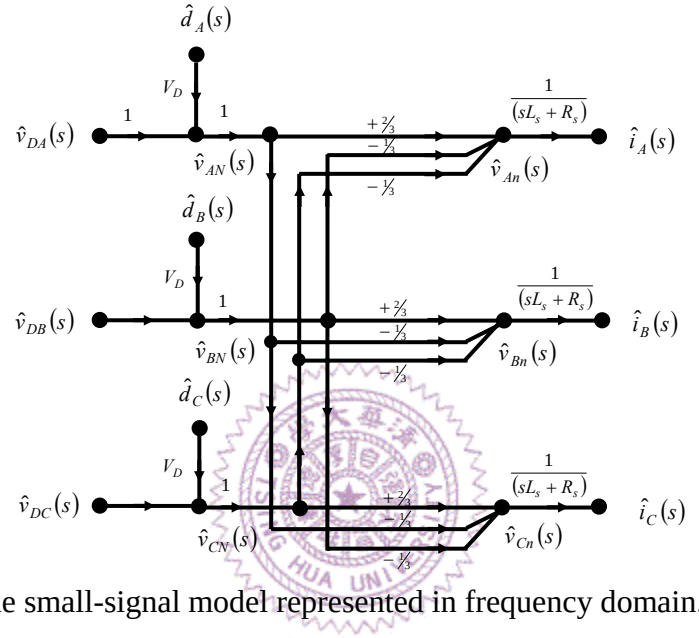

Fig. 5.7 The small-signal model represented in frequency domain.

From Fig. 5.11 one can easily find the transfer functions $\hat{d}_j(s)/\hat{i}_k(s)$ for $j,k \in \{A,B,C\}$ by using Mason's Rule.

$$\frac{\hat{d}_j(s)}{\hat{i}_k(s)} = \begin{cases} \dfrac{2}{3}V_D\dfrac{1}{(sL_s+R_s)} & \text{for} \quad j=k \\ -\dfrac{1}{3}V_D\dfrac{1}{(sL_s+R_s)} & \text{for} \quad j\neq k \end{cases} \tag{5.7}$$
$$j,k \in \{A,B,C\}$$

According to equation (5.9) the PI-controllers for each phase of the inverters can be designed as follows:

$$G_{jk}(s) = \begin{cases} h_{jj}\dfrac{3}{2V_D}\left(\dfrac{R_s}{s}+L_s\right) & \text{for} \quad j=k \\ -h_{jk}\dfrac{3}{V_D}\left(\dfrac{R_s}{s}+L_s\right) & \text{for} \quad j\neq k \end{cases} \tag{5.8}$$
$$j,k \in \{A,B,C\}$$

where the h_{jk} is the bandwidth of the controllers. In this example, the bandwidth of the current controllers is chosen as $1/5$ switching frequency; that is, h_{jk} equals to $400\pi\ rad$ for switching frequency f_S is *1 kHz*. Therefore, the current controllers can be represented as following.

$$G_{jk}(s)=\begin{cases}14\left(\dfrac{3.55}{s}+0.00592\right) & \text{for} \quad j=k\\ -28\left(\dfrac{3.55}{s}+0.00592\right) & \text{for} \quad j\neq k\end{cases} \qquad (5.9)$$
$$j,k\in\{A,B,C\}$$

The current controllers for A-phase can be implemented with MATLAB/SIMULINK as depicted in the Fig. 5.12. Fig. 5.12 can be used as a controller cell and can easily be applied to each phase. The whole simulation structure is shown in Fig. 5.13, that includes the proposed SFG model of inverters (described in Fig. 3.11), the simulation model of SMPMSM (Fig. 5.3), speed regulator [44], bound calculator [44], axis transformers and current controllers (Fig. 5.12).

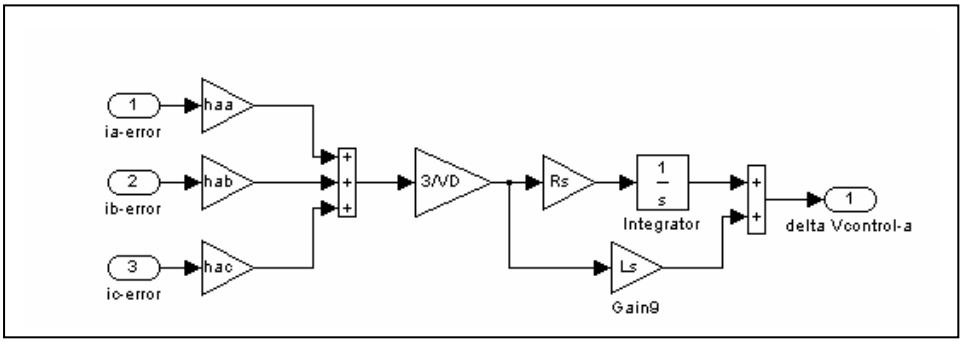

Fig. 5.8 The A-phase current controllers implemented with MATLAB/SIMULINK.

In this case, the maximum phase voltage magnitude and maximum phase current magnitude of the inverter are $100V$ and $2A$ respectively. The motor is started from zero speed and the original speed setpoint is +2400 *rpm*. Then the speed target is changing to -2400 *rpm* and 0 at 0.1 *sec* and 0.24 *sec* respectively. Fig. 5.14 reveals the

simulation waveforms of stators currents i_d, i_q, torque and rotor speed for f_S is *1 kHz*. When f_S is increased to *10 kHz*, the current controllers can be modified as:

$$G_{jk}(s)=\begin{cases} 140\left(\dfrac{3.55}{s}+0.00592\right) & \text{for} \quad j=k \\ -280\left(\dfrac{3.55}{s}+0.00592\right) & \text{for} \quad j\neq k \end{cases} \qquad (5.10)$$
$$j,k\in\{A,B,C\}$$

The simulation results are shown in Fig. 5.15.

This example demonstrates how to design the current controllers by using the small-signal SFG model. This example also provides a system-level simulation structure for general motor system. Actually, the proposed SFG model of the inverters can be regarded as a built-in subsystem and can be used for different applications. One can reconstruct the motor's model according to different requirement. Furthermore, the various kinds of controllers, like fuzzy controllers or sliding-mode controllers, can easily be implemented with this simulation structure.

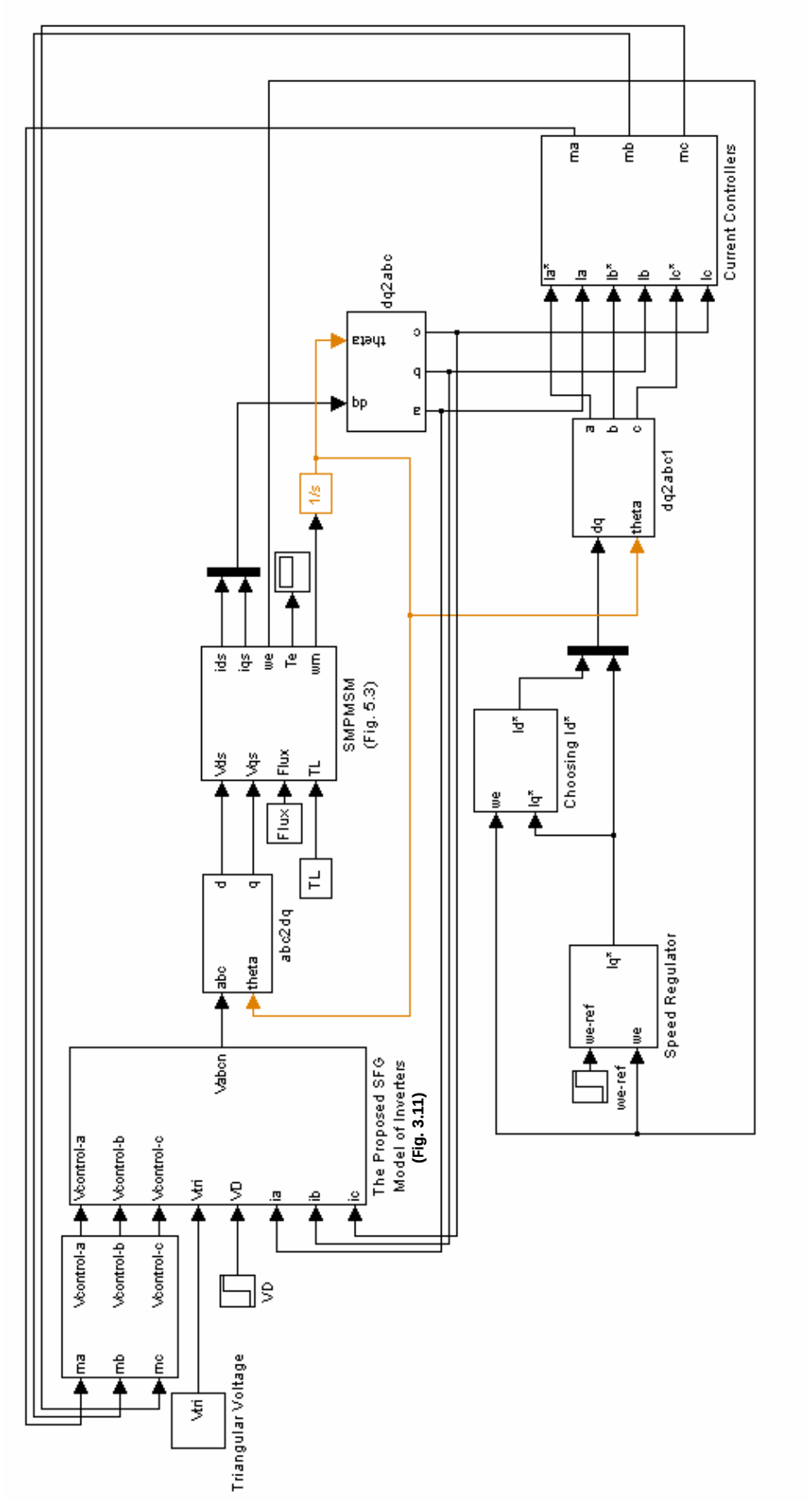

Fig. 5.9 The simulation model of the motor system with the proposed SFG model.

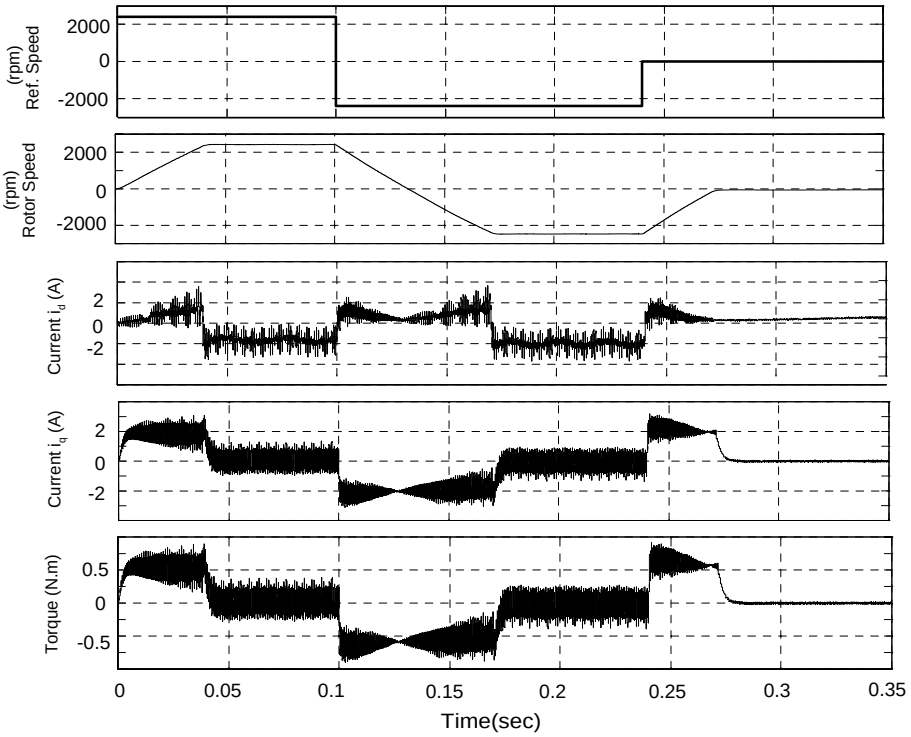

Fig. 5.10 The simulation waveforms of the stators currents i_d, i_q, torque and rotor speed for $f_S = 1kHz$.

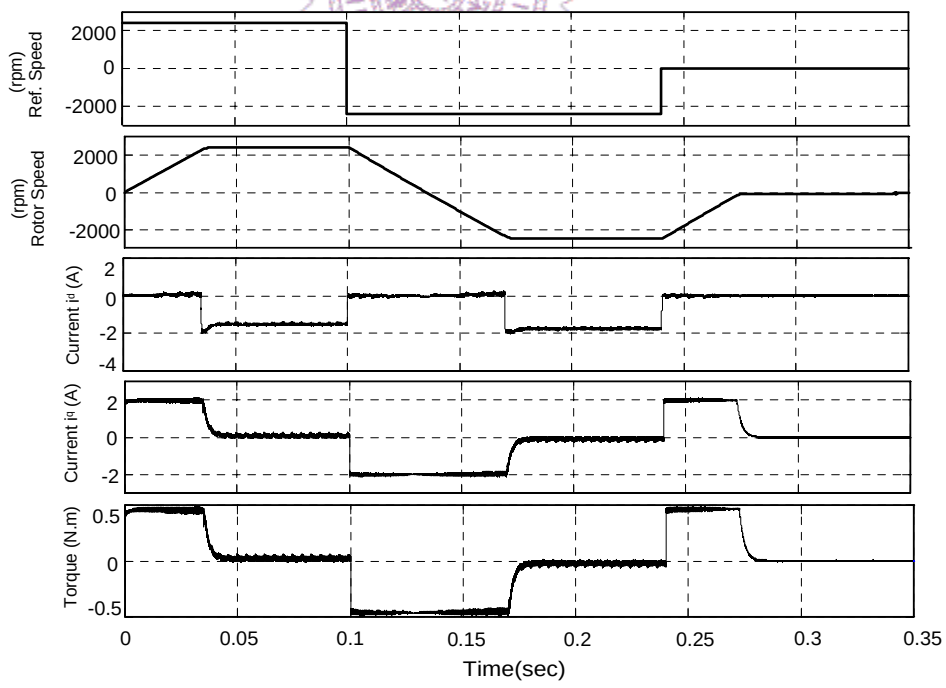

Fig. 5.11 The simulation waveforms of the stators currents i_d, i_q, torque and rotor speed for $f_S = 10kHz$.

5.3 Application Examples of Rectifiers

5.3.1 Simplified SFG Model for Diode-Rectifier Simulation

It is very easy to get the simulation model of the full-bridge diode rectifier from the SFG model of three-phase rectifiers. From equation (4.3) ~ (4.8), one can find that the virtual switching functions and diode switching functions are developed by the combination of the original switching functions and the judgment of current directions. Therefore, if the switching functions $F_{S_{jP}}(t)$ and $F_{S_{jN}}(t)$, $j \in \{A,B,C\}$, are set to be zero, that means all the switches are operated under the OFF state, the remnants of virtual switching functions will be the switching functions of diodes. Hence, the simulation model of the full-bridge diode rectifier can be obtained directly by setting $F_{S_{jP}}(t)$ and $F_{S_{jN}}(t)$, $j \in \{A,B,C\}$ to be zero.

Consider a typical full-bridge diode rectifier as shown in Fig. 5.16, where the conditions of AC voltage source and the passive components are the same as used in section 4.4. The waveforms of output voltage and AC current are depicted in Fig. 5.17 and Fig. 5.18, respectively. One can see that the simulation results generated from SFG model are in close agreement with that generated from PSPICE. However, the execution time of using the proposed SFG model is only 1/10 of that by using PSPICE model. This model is very helpful for simulation of a wind energy system.

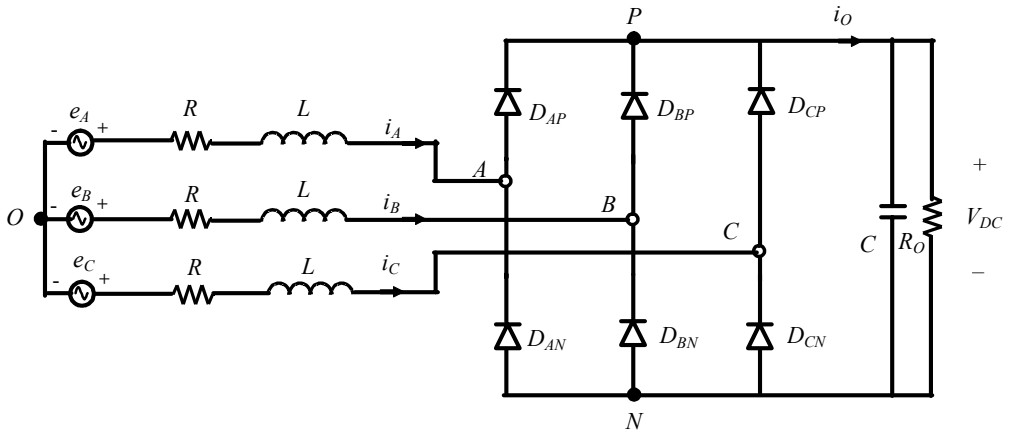

Fig. 5.12 The circuit configuration of the full-bridge diode rectifier.

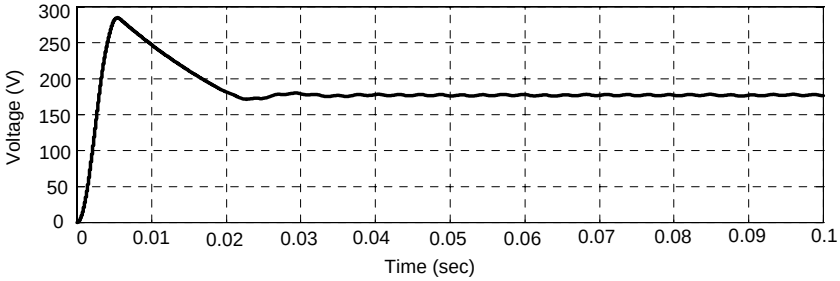

(a)

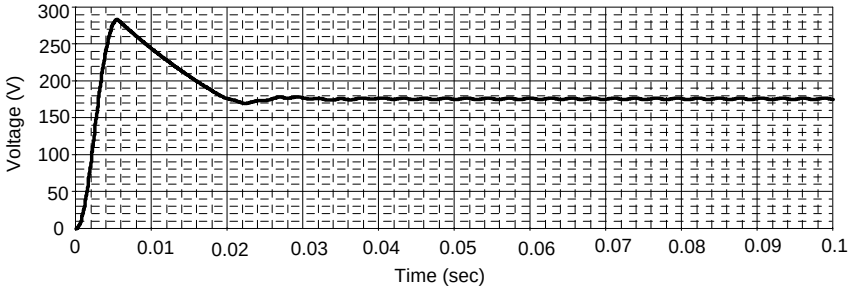

(b)

Fig. 5.13 The Simulation results of the output voltage using (a) proposed SFG model, (b) PSPICE model.

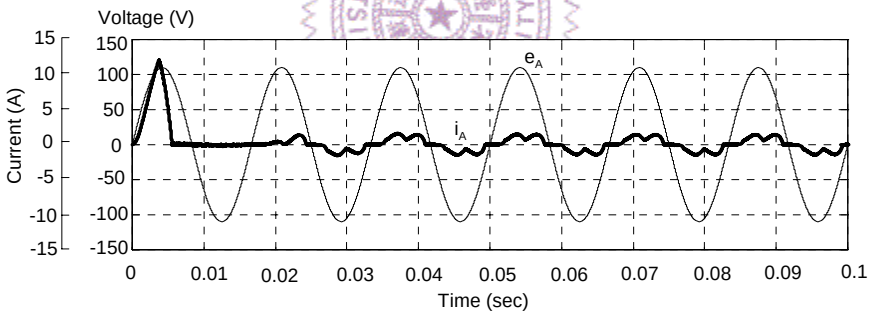

(a)

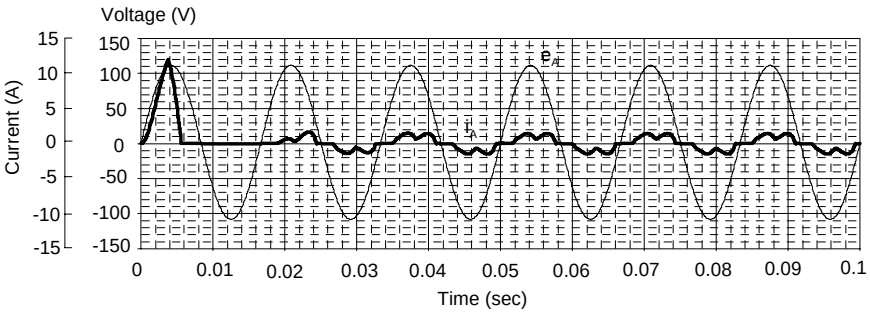

(b)

Fig. 5.14 The Simulation results of the AC current and voltage of A-phase using (a) proposed SFG model, (b) PSPICE model.

5.3.2 The SFG Model for Three-Phase Rectifier with Unbalanced Input Sources

When the three-phase rectifier operated with unbalanced input sources, one can obtain $v_{NO}(t)$ from equation (4.10), as shown in equation (5.11).

$$v_{NO} = \tfrac{1}{3}\left(e_A(t)+e_B(t)+e_C(t)\right)-\tfrac{1}{3}\left(F_A(t)+F_B(t)+F_C(t)\right)V_{DC} \tag{5.11}$$

According to equation (5.11), equation (4.13) can be rewritten as:

$$e_A = Ri_A + L\frac{di_A}{dt}+\left(\tfrac{2}{3}F_A-\tfrac{1}{3}F_B-\tfrac{1}{3}F_C\right)V_{DC}+\tfrac{1}{3}\left(e_A+e_B+e_C\right) \tag{5.12a}$$

$$e_B = Ri_B + L\frac{di_B}{dt}+\left(\tfrac{2}{3}F_B-\tfrac{1}{3}F_A-\tfrac{1}{3}F_C\right)V_{DC}+\tfrac{1}{3}\left(e_A+e_B+e_C\right) \tag{5.12b}$$

$$e_C = Ri_C + L\frac{di_C}{dt}+\left(\tfrac{2}{3}F_C-\tfrac{1}{3}F_B-\tfrac{1}{3}F_A\right)V_{DC}+\tfrac{1}{3}\left(e_A+e_B+e_C\right) \tag{5.12c}$$

Therefore, inserting the part of $\tfrac{1}{3}\left(e_A(t)+e_B(t)+e_C(t)\right)$ into Fig. 4.6, the large-signal model can easily be obtained as depicted in Fig. 5.15.

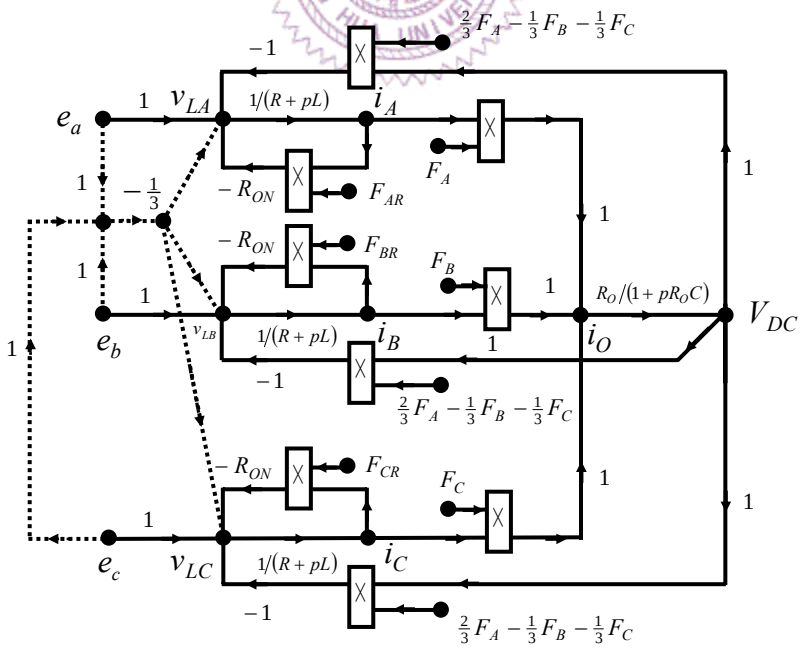

Fig. 5.15 The large-signal model for three-phase rectifiers with unbalanced input sources.

In Fig. 5.15, the dotted branches represent the part of $-\tfrac{1}{3}\left(e_A(t)+e_B(t)+e_C(t)\right)$ that is

added to the node variable $v_{Lj}(t)$, $j \in \{A,B,C\}$.

Similarly, one can implement the large-signal model with MATLAB/SIMULINK to execute the time-domain simulation.

5.3.3 PI-Controller Design for Rectifiers by Using the Proposed SFG Model

This section introduces how to use the SFG model to design the PI-controllers with the concept of IMC (internal model control) for the three-phase rectifiers. The rectifier drawn in Fig. 4.1 is used as the example. The PI-controllers and the proposed SFG model are implemented with MATLAB/SIMULINK to estimate the transient and steady-state behavior of whole system.

A. Structure of Control System

The control structure of the three-phase rectifier is depicted in Fig. 5.16. From Fig. 5.16, one can observe that the actuation signals of the three-phase rectifier are the virtual switching functions $F_A(t)$, $F_B(t)$ and $F_C(t)$, and input sources $e_A(t)$, $e_B(t)$ and $e_C(t)$. The output signals of the control system are the DC voltage V_O and phase currents $i_A(t)$, $i_B(t)$ and $i_C(t)$. In this example, the control target of the output voltage is V_{O-ref}. There are one voltage controller $G_V(s)$ and two current controllers $G_{id}(s)$ and $G_{iq}(s)$; where each controller has the anti-windup design to prevent the phenomenon of integral windup. There are also two blocks of coordinate –conversion, with symbol of X32 and X23, in the control structure to make the transformation from abc- axis (dq-axis) to dq-axis (abc-axis). The block symbolized XG is a gain block, that transfers the duty ratios $d_A(t)$, $d_B(t)$ and $d_C(t)$ to the control voltages $V_{A-control}(t)$, $V_{B-control}(t)$ and $V_{C-control}(t)$. In XC block, the control voltages are compared with the triangular voltage V_{tri} to generate the switching functions for six active switches. Then, the virtual switching functions $F_A(t)$, $F_B(t)$ and $F_C(t)$ can be created as described in Fig. 4.3. The XP-block is the proposed SFG model of the three-phase rectifier as shown in Fig. 4.6.

B. Controller Design

From Fig. 4.9b, on can obtain the transfer functions easily by using Mason's Rule. In this example the voltage controller and the current controllers are designed separately. Therefore, the transfer functions of $\frac{\hat{v}_{DC}(s)}{\hat{i}_d(s)}$, $\frac{\hat{v}_{DC}(s)}{\hat{i}_q(s)}$, $\frac{\hat{i}_d(s)}{\hat{d}_d(s)}$, $\frac{\hat{i}_d(s)}{\hat{d}_q(s)}$, $\frac{\hat{i}_q(s)}{\hat{d}_d(s)}$ and $\frac{\hat{i}_q(s)}{\hat{d}_q(s)}$ are required to be derived out for the controller design. In order to clearly explain how to get the transfer functions straightforward from the small-signal SFG model, the model can be redrawn as Figs. 5.17 and 5.18; where the branches plotted with dotted line are ineffective branches.

In Fig. 5.17, the input nodes and output node are $\hat{i}_d(s)$, $\hat{i}_q(s)$ and $\hat{v}_{DC}(s)$ respectively and the other input sources are set to be zero. Therefore, by using the Mason's Rule, the transfer functions of $\frac{\hat{v}_{DC}(s)}{\hat{i}_d(s)}$ and $\frac{\hat{v}_{DC}(s)}{\hat{i}_q(s)}$ can be written as equations (5.13) and (5.14) from Fig. 5.17

$$\frac{\hat{v}_{DC}(s)}{\hat{i}_d(s)} = \frac{D_d R_O}{(1+sCR_O)} \tag{5.13}$$

$$\frac{\hat{v}_{DC}(s)}{\hat{i}_q(s)} = \frac{D_q R_O}{(1+sCR_O)} \tag{5.14}$$

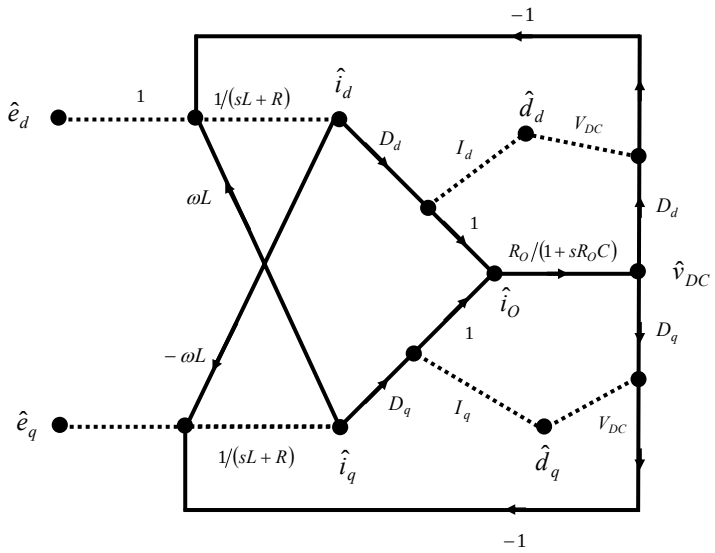

Fig. 5.17 The small-signal SFG model for finding out the transfer functions of $\frac{\hat{v}_{DC}(s)}{\hat{i}_d(s)}$ and $\frac{\hat{v}_{DC}(s)}{\hat{i}_q(s)}$.

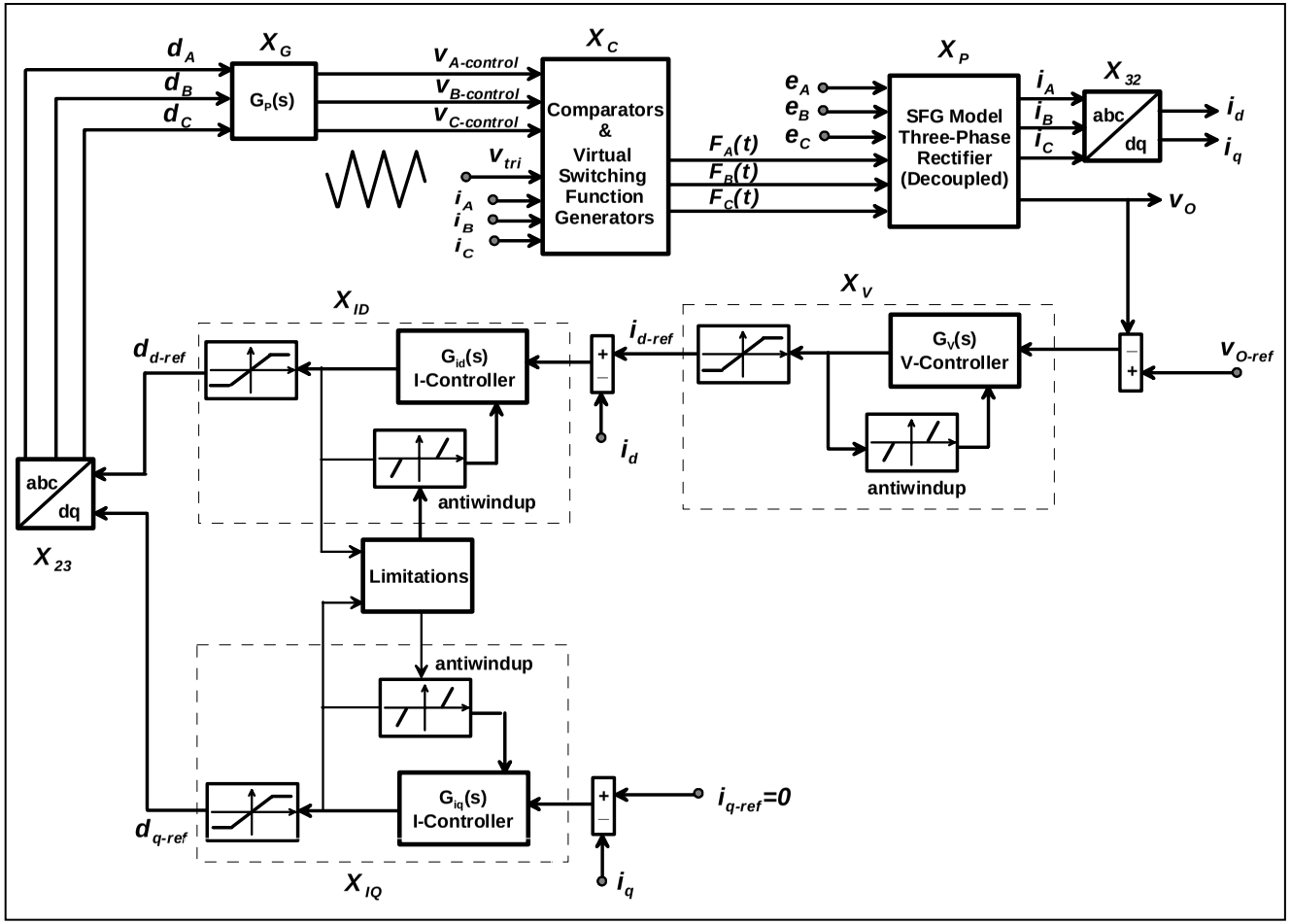

Fig. 5.16 The control structure for the three-phase rectifier.

Similarly, the transfer functions of $\frac{\hat{i}_d(s)}{\hat{d}_d(s)}$, $\frac{\hat{i}_d(s)}{\hat{d}_q(s)}$, $\frac{\hat{i}_q(s)}{\hat{d}_d(s)}$ and $\frac{\hat{i}_q(s)}{\hat{d}_q(s)}$ can be written as follows from Fig. 5.18:

$$\frac{\hat{i}_d(s)}{\hat{d}_d(s)} = \frac{\frac{-V_{DC}}{(sL+R)}}{p(s)} \tag{5.15}$$

$$\frac{\hat{i}_d(s)}{\hat{d}_q(s)} = \frac{\frac{-V_{DC}\omega L}{(sL+R)^2}}{p(s)} \tag{5.16}$$

$$\frac{\hat{i}_q(s)}{\hat{d}_d(s)} = \frac{\frac{V_{DC}\omega L}{(sL+R)^2}}{p(s)} \tag{5.17}$$

$$\frac{\hat{i}_q(s)}{\hat{d}_q(s)} = \frac{\frac{-V_{DC}}{(sL+R)}}{p(s)} \tag{5.18}$$

where $p(s) = 1 + \frac{(\omega L)^2}{(sL+R)^2}$

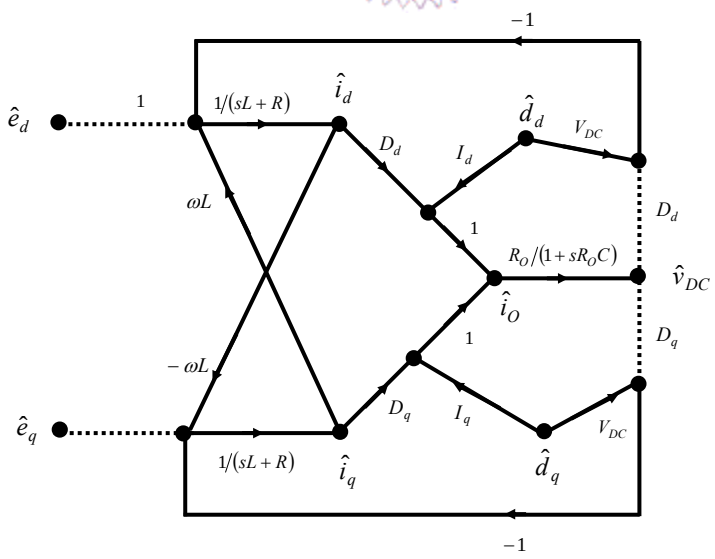

Fig. 5.18 The small-signal SFG model for finding out the transfer functions of $\frac{\hat{i}_d(s)}{\hat{d}_d(s)}$, $\frac{\hat{i}_d(s)}{\hat{d}_q(s)}$, $\frac{\hat{i}_q(s)}{\hat{d}_d(s)}$ and $\frac{\hat{i}_q(s)}{\hat{d}_q(s)}$.

Then, according to the design concept of internal model control (IMC) [46], [47], the voltage controller $G_v(s)$ and current controllers $G_{id}(s)$ and $G_{iq}(s)$ can be described as:

$$G_{id}(s)=\frac{\alpha_i}{s}\left(\frac{\hat{i}_d(s)}{\hat{d}_d(s)}\right)^{-1}=\frac{\alpha_{id}}{s}\left(\frac{-L}{V_{DC}}\left(s+\frac{R}{L}\right)\right) \tag{5.19}$$

$$G_{iq}(s)=\frac{\alpha_i}{s}\left(\frac{\hat{i}_q(s)}{\hat{d}_q(s)}\right)^{-1}=\frac{\alpha_{iq}}{s}\left(\frac{-L}{V_{DC}}\left(s+\frac{R}{L}\right)\right) \tag{5.20}$$

$$G_v(s)=\frac{\alpha_v}{s}\left(\frac{\hat{v}_{DC}(s)}{\hat{i}_d(s)}\right)^{-1}=\frac{\alpha_v}{s}\left(\frac{C}{D_d}\left(s+\frac{1}{CR_O}\right)\right) \tag{5.21}$$

where α_{id}, α_{iq}, and α_v are the desired closed-loop bandwidths.

In addition, from equations (5.16) and (5.17), the decoupling matrix $W(s)$ can be written as (5.22), which is used as an inner feedback loop to remove the cross coupling of the control plan [46], [47].

$$W(s)=\begin{bmatrix}0 & -\omega L\\ \omega L & 0\end{bmatrix} \tag{5.22}$$

Appendix A describes the design procedure of using the conventional model. One can observe that the controllers designed by using the proposed SFG model are the same as that by using the equation-form model. However, by using the conventional model to design the controllers require more mathematic work. Obviously, it is easier by using the proposed SFG model to design the controllers.

C. Simulation Results

Consider the example as shown in Fig. 4.1 where $R_O=110\Omega$, $C=220\mu F$, $R_{ON}=0.23\Omega$, $R=0.12\Omega$ and $L=3.5mH$. The AC sources are set to be:

$$e_A(t) = 50\cos(120\pi t)$$
$$e_B(t) = 50\cos(120\pi t - 120^\circ)$$
$$e_C(t) = 50\cos(120\pi t + 120^\circ)$$

Assume the well known sinusoidal PWM is adopted. The switching frequency of the rectifier is $f_S = 20kHz$ and the amplitude of the triangular wave is $1V$. The rated power of the system is $750W$. The dc-voltage reference is 150V and the rated load current is $5A$. According to the steady-state SFG model revealed in Fig. 4.8, the working point of the rectifier can be obtained:

$$D_d^* = 0.4055,\quad D_q^* = -0.03,\quad I_d^* = 3.4,\quad I_q^* = 0.$$

From equations (5.19) ~ (5.21), the controllers can be described in equations (5.23) ~ (5.25).

$$G_{id}(s) = \frac{-0.59}{s}(s + 34.3) \tag{5.23}$$
$$G_{iq}(s) = \frac{-0.59}{s}(s + 34.3) \tag{5.24}$$
$$G_v(s) = \frac{1}{s}(s + 41.3) \tag{5.25}$$

According to the Fig. 5.19, the whole control system can be implemented with MATLAB/SIMULINK to execute the time-domain simulation. The simulation model built in MATLAB/SIMULINK environment is depicted in Fig. 5.19. The output load R_O is changed to 220Ω at $0.1sec$ and the voltage command is changed to $180V$ at $0.2sec$. The waveforms of the dc-voltage and the phase currents are both shown in Fig. 5.20 as simulated with controllers.

This example demonstrates that the proposed SFG model supplies a simple way to design the controllers without laborious mathematics. The graphic representation of the model renders more physical insight of the control structure that is really helpful for the controller design.

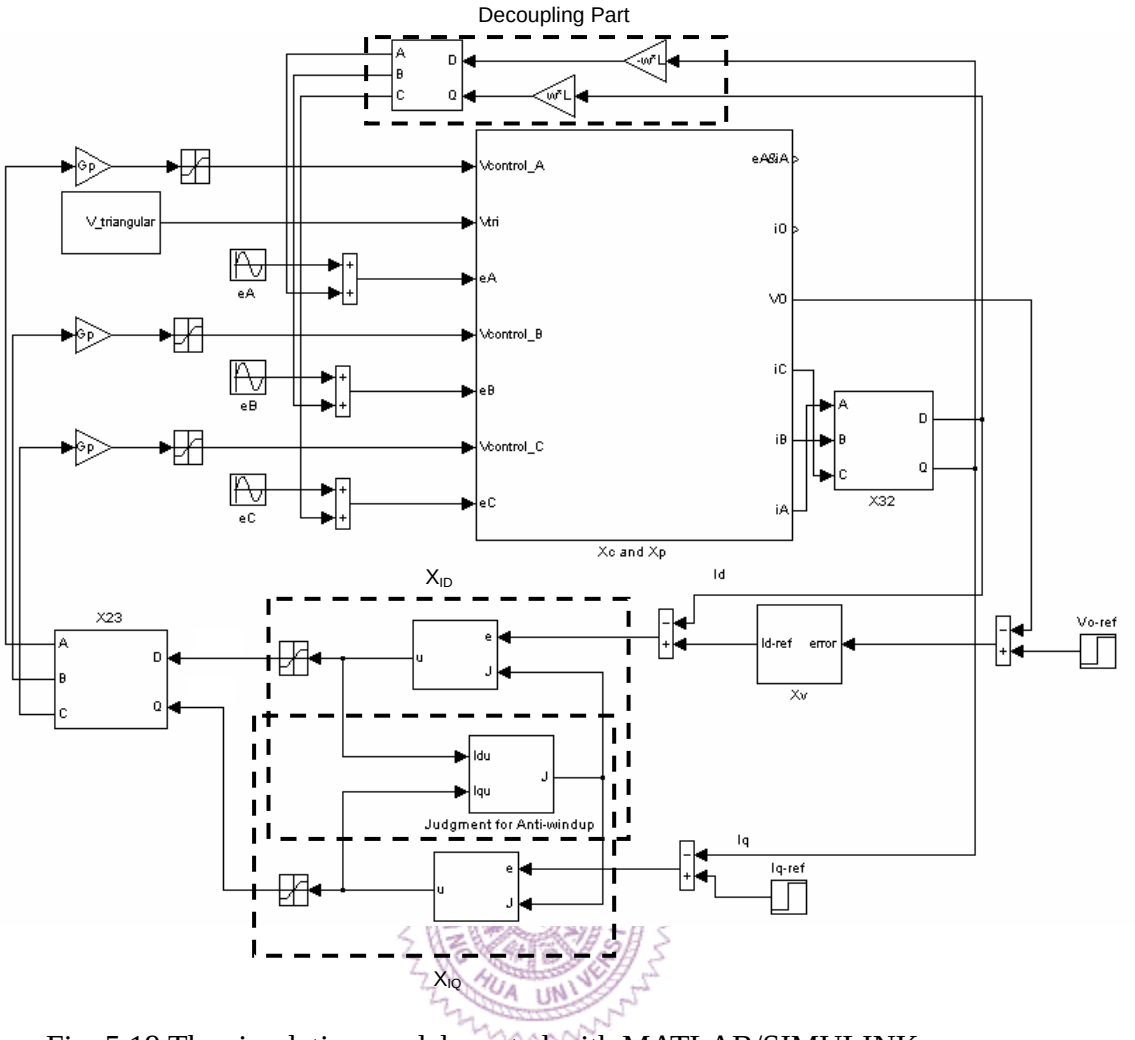

Fig. 5.19 The simulation model created with MATLAB/SIMULINK.

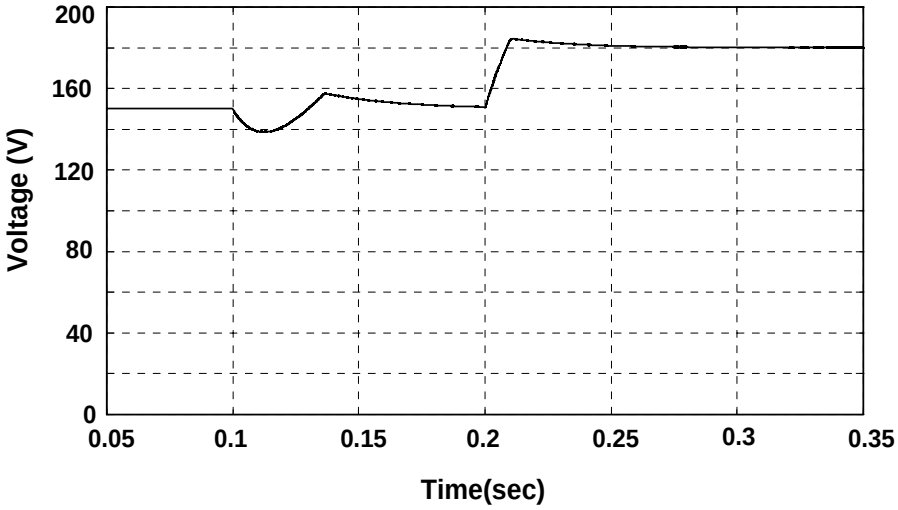

(a)

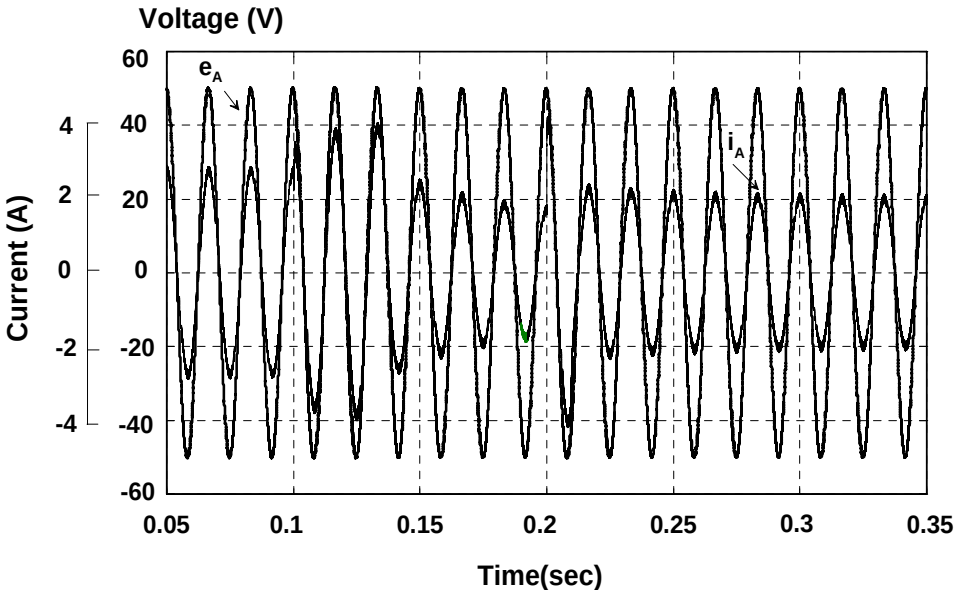

(b)

Fig. 5.20 The simulation results of (a) the output voltage, (b) the AC current and voltage of A-phase with controllers.

These application examples show that the proposed SFG modeling technique provides unified large-signal model, steady-state model and small-signal model of three-phase switching converters. The proposed SFG model is more computationally efficient for system-level simulation as compare with the PSPICE model. It is very easy to analyze the switching systems and to design the controllers by using the proposed SFG model. Nevertheless, the proposed SFG model can be directly implemented with SIMULINK/MATLAB and correctly predict the transient and steady-state response.